LA-UR- 01-1031

c.1

*Approved for public release; distribution is unlimited.*

*Title:* OBSERVING SINGLE MOLECULE CHEMICAL REACTIONS ON METAL NANOPARTICLES

*Author(s):* Steven R. Emory B-N2
W. Patrick Ambrose B-N2
Peter M. Goodwin B-N2
Richard A. Keller B-N2

*Submitted to:* Proceedings of the SPIE



**Los Alamos**
NATIONAL LABORATORY

# Observing single molecule chemical reactions on metal nanoparticles

Steven R. Emory, W. Patrick Ambrose, Peter M. Goodwin, and Richard A. Keller

Bioscience Division, Los Alamos National Laboratory, MS M888, Los Alamos, NM 87545

## ABSTRACT

We report the study of the photodecomposition of single Rhodamine 6G (R6G) dye molecules adsorbed on silver nanoparticles. The nanoparticles were immobilized and spatially isolated on polylysine-derivatized glass coverslips, and confocal laser microspectroscopy was used to obtain surface-enhanced Raman scattering (SERS) spectra from individual R6G molecules. The photodecomposition of these molecules was observed with 150-ms temporal resolution. The photoproduct was identified as graphitic carbon based on the appearance of broad SERS vibrational bands at 1592 $cm^{-1}$ and 1340 $cm^{-1}$ observed in both bulk and averaged single-molecule photoproduct spectra. In contrast, when observed at the single-molecule level, the photoproduct yielded sharp SERS spectra. The inhomogeneous broadening of the bulk SERS spectra is due to a variety of photoproducts in different surface orientations and is a characteristic of ensemble-averaged measurements of disordered systems. These single-molecule studies indicate a photodecomposition pathway by which the R6G molecule desorbs from the metal surface, an excited-state photoreaction occurs, and the R6G photoproduct(s) readsorbs to the surface. A SERS spectrum is obtained when either the intact R6G or the R6G photoproduct(s) are adsorbed on a SERS-active site. This work further illustrates the power of single-molecule spectroscopy (SMS) to reveal unique behaviors of single molecules that are not discernable with bulk measurements.

**Keywords:** surface-enhanced Raman scattering (SERS), nanoparticles, single-molecule detection (SMD), single-molecule spectroscopy (SMS), Rhodamine 6G (R6G).

## 1. INTRODUCTION

There have been many recent reports of surface-enhanced Raman scattering (SERS) at the single-molecule level. These new results have generated considerable excitement in both the Raman and single-molecule spectroscopy communities.[1] The observed enhancement factors are on the order of $10^{14}$ to $10^{15}$,[2-5] which are much larger than ensemble-averaged values ($10^6$ to $10^8$) obtained with conventional SERS measurements[6]. Both electromagnetic and chemical enhancement mechanisms have been proposed to explain the SERS phenomenon.[6] An additional finding of these new studies is the presence of optically "hot" nanoparticles that are highly efficient for surface enhancement.[2-5,7] Raman scattering from these optically "hot" nanoparticles occurs intermittently.[2,4,5] This blinking behavior is similar in appearance to discontinuous fluorescence emission observed for single dye molecules[8-10] and single semiconductor quantum dots,[11-13] but the fundamental mechanisms have yet to be definitively determined in many cases. By probing one nanoparticle at a time, these studies have overcome the effects of ensemble averaging and have revealed the intrinsic properties associated with single nanoparticles.

A major advantage of single-molecule detection (SMD) and spectroscopy (SMS) is the ability to reveal events masked by ensemble-averaging inherent in bulk measurements. Various groups have successfully exploited this using laser-induced fluorescence (LIF) to study single-molecule photodynamics, photochemistry, and molecular dynamics.[8-10,14-20] An extension of these studies is to follow a complete chemical reaction at the single-molecule level. This has been accomplished to a limited degree by LIF. For example, the photobleaching of fluorescent molecules such as B-phycoerythrin,[17] R6G,[18,19] and allophycocyanin trimers[20] have been studied. However, SMD by LIF is limited to the study of highly fluorescent molecules and often does not provide sufficient spectral information for chemical identification. In the case of photobleaching, only the disappearance of the analyte is observed and the identity of the

Further author information:
S.R.E. (correspondence): E-mail: semory@lanl.gov; Telephone: (505) 665-2092; Fax: (505) 665-3024
W.P.A.: E-mail: wpa@lanl.gov; Telephone: (505) 665-2092; Fax: (505) 665-3024
P.M.G: E-mail: pmg@lanl.gov; Telephone: (505) 665-2092; Fax: (505) 665-3024
R.A.K.: E-mail: keller@lanl.gov; Telephone: (505) 667-3018; Fax (505) 665-3024

nonfluorescent photoproduct(s) must be determined by other means. An ideal SMD method would allow the detection and identification of both the reactant and product molecules. Single-molecule SERS spectroscopy has the potential to provide such information via a vibrational fingerprint and, unlike LIF, does not require the analyte to be fluorescent.

In this work, we take advantage of the single-molecule sensitivity and structural information provided by SERS to follow the photodecomposition reaction of individual R6G molecules adsorbed on silver nanoparticles. In the case of R6G, there is an abundance of SERS studies in the literature including studies at the single-molecule level.[1] Photochemistry of molecules adsorbed on metal surfaces, such as silver, has also been studied extensively by SERS. In some cases, surface-enhanced photochemistry has been observed. The concept of surface-enhanced photochemistry was first outlined by Nitzan and Brus[21] and has since been extended by other groups.[22,23] Experimental studies, lead by Moskovits and coworkers,[24] have reported this phenomenon for a wide range of adsorbed species.[24-26] The fundamental conclusion is that the same electromagnetic field enhancement involved in SERS is also capable of enhancing photochemical reactions on SERS-active substrates. Experimental and theoretical studies have determined the most efficient location for surface-enhanced photochemistry is not on the metal surface, but rather a short distance away from the surface. Although the electromagnetic field decreases as a function of distance from the surface, the excited-state lifetime increases as the molecule moves away. Therefore, at a position slightly above the surface, a maximum photochemical rate can be reached where the two competing effects are balanced. In the case of R6G, the increased photostability on metal surfaces was attributed to efficient nonradiative damping of electronic excited states.[18,27] However, as is described in this report, R6G does undergo photodecomposition on silver nanoparticles, albeit at a reduced rate. Our single-molecule SERS data provides important new information that aids in understanding the photodecomposition and blinking mechanisms observed for R6G on silver.

## 2. EXPERIMENTAL

### 2.1 Materials

Silver nitrate (analytical grade, Aldrich), sodium citrate (analytical grade, Fisher), sodium chloride (biological grade, Fisher), Rhodamine 6G perchlorate (Molecular Probes), and poly-L-lysine hydrobromide (molecular weight 2.5 x $10^6$ g/mole, Sigma) were used as received. Ultrapure water (18 MΩ·cm, Millipore) was used to prepare all aqueous solutions. Pure ethanol (99+%, Quantum Chemical) was used for diluting the R6G stock solution. Glass microscope coverslips (No. 1, 25 x 25 mm, Corning) were cleaned in concentrated sulfuric acid for approximately one minute, rinsed with copious amounts of ultrapure water, and dried with nitrogen.

### 2.2 Colloidal Silver Synthesis

The silver colloid was prepared by the citrate reduction method outlined by Lee and Meisel.[28] Colloid concentration was determined to be 3 x $10^{11}$ nanoparticles/mL and the absorbance spectrum showed a maximum at ~420 nm, characteristic of ~35 nm diameter silver nanoparticles. The colloid was stored in a sealed Erlenmeyer flask and was stable for several months.

### 2.3 Preparation of Samples for Single-Molecule SERS Studies

For single-molecule studies, a 5-μL aliquot of 1 nM R6G in ethanol was added directly to 250 μL of silver colloid in a 500-μL polypropylene microcentrifuge tube. This corresponds to ~0.1 R6G molecules per nanoparticle. The mixture was immediately mixed with a pipette and then vortexed for approximately 10 seconds. After 10 minutes, 9.4 μL of 20 mM sodium chloride was added and mixed to activate the colloid as described in previous studies.[2,29] The R6G/colloid mixture was allowed to incubate at room temperature for at least 30 minutes prior to immobilization on polylysine-coated glass coverslips for analysis.

The nanoparticles were immobilized on polylysine-coated glass coverslips using the following procedure:[2,7] 5 μL of the R6G/colloid mixture was placed on a polylysine-coated glass coverslip (~2 nanoparticles per $\mu m^2$). An uncoated glass coverslip was used to spread evenly the solution between the two coverslips. The negatively charged nanoparticles (the citrate that stabilizes the colloid is negatively charged) electrostatically bind to the positively charged surface. After approximately 10 minutes, the two coverslips were pulled apart. The polylysine-coated coverslip was then air-dried prior to analysis. A majority of the nanoparticles was sufficiently spatially isolated (>1 μm apart) to allow far-field microscopy to interrogate single nanoparticles or nanoaggregates (2 to 5 nanoparticles) at a time. The sample was then positioned on the microscope stage (Section 2.5) for analysis, and no further characterization was performed to determine if single nanoparticles or nanoaggregates were probed.

## 2.4 Preparation of Samples for Ensemble-Averaged SERS Studies

More concentrated samples for ensemble-averaged measurements were prepared in the same manner as described for single-molecule SERS samples (Section 2.3) with the following changes: a 5-μL aliquot of 10 μM R6G in ethanol was added to the colloid (to yield ~1000 R6G molecules per nanoparticle); 20 μL of the R6G/colloid mixture was placed and air-dried onto a polylysine-coated coverslip with a spot diameter of approximately 5 mm. This corresponds to a density of approximately 300 nanoparticles per $\mu m^2$. The sample was then positioned on the microscope stage (Section 2.5) for analysis.

## 2.5 Instrumentation

A confocal Raman microscope was constructed to obtain SERS spectra from single isolated nanoparticles or nanoaggregates (Figure 1). The 514.5-nm laser line from an argon ion laser (Innova 90, Coherent) was used for excitation. Approximately 5 mW of laser light was focused to a spot ~600 nm in diameter[30] yielding an irradiance of 2 $MW/cm^2$ or 5 x $10^{24}$ photons/($s \cdot cm^2$). A mechanical shutter (SH) was used to minimize laser-induced damage to the sample when spectra were not being collected. A laser line notch-filter (F1, 514LF, Omega Optical) was used to filter the

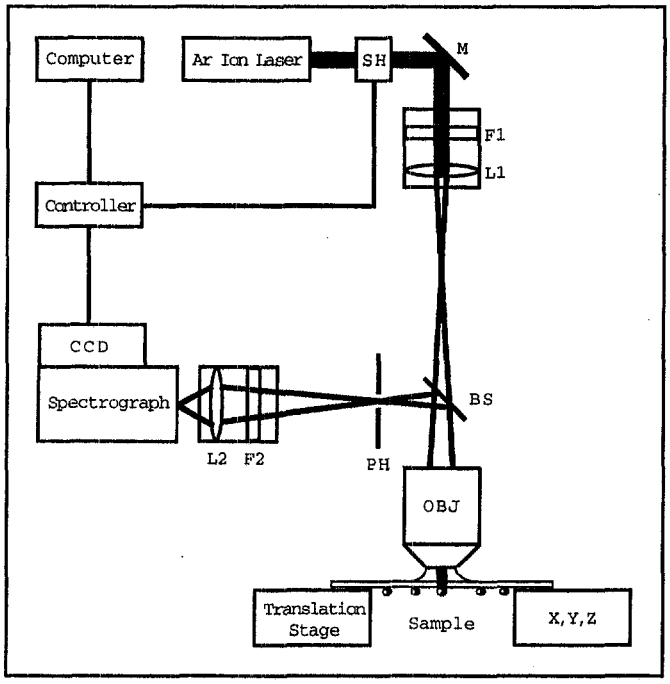


**Figure 1.** Diagram of confocal Raman microscope. See text for discussion.

background from the plasma discharge. An achromatic, plano-convex focusing lens (L1, f = 150 mm, aperture = 21.5 mm, Melles Griot) was used to expand the beam to fill the back aperture of an oil immersion objective (100x, 1.1NA, Zeiss). The sample coverslip was mounted horizontally on an x,y,z-translation stage using Scotch™ tape. Immersion oil (Type DF, $\eta_D$ = 1.5150 +/- 0.0002, Cargille) was placed directly between the objective and the glass coverslip. Stokes-shifted Raman light was collected in an epi-illumination geometry. A dichroic reflector (BS, 525DRSP, Omega Optical) directed the collected light to a pinhole (PH, diameter = 1 mm) for stray-light rejection. An angle-tunable holographic Raman notch filter (F2, HSPF-515.5-1.0, Kaiser Optical) filtered out the reflected or Rayleigh backscattered excitation photons. An aspheric lens (L2, C220TM-A, f = 11.0 mm, 0.25NA, Thorlabs) focused the light onto the entrance slit (500 μm) of a high-throughput imaging spectrograph (f-number = 2.2, Holospec, Kaiser Optical). Spectra were acquired with a thermoelectrically-cooled CCD camera (Model number TWA/CCD-1242-EM-1, Roper Scientific [formerly Princeton Instruments]) operated at 1 MHz (12 bits) and optimized for rapid spectral acquisition. Spectra were processed with *Winspec* software (v. 1.6, Princeton Instruments). A 100 x 1152 strip was selected out of the total 1242 x 1152 pixel CCD chip. The pixels where the analyte spectrum was focused (10 x 1152) were binned vertically to a final configuration of 1 x 1152. The detector readout time was measured with an oscilloscope to be 50 ms. An integration time of 100 ms was necessary to acquire single-molecule SERS spectra with reasonable signal to noise. Thus for a given spectrum, a total of 150 ms (100 ms integration plus 50 ms deadtime readout) was required for spectral acquisition. CCD detector counts were converted to photoelectrons (pe) by multiplying by 35 photoelectrons/count (manufacturer's

specification). For displayed spectra, intensity was calculated as pe/(s·bin) obtained by dividing the pe/bin by the integration time.

## 3. RESULTS

### 3.1 Ensemble-Averaged SERS Spectra

Figure 2 shows the photodecomposition SERS spectra of an ensemble of R6G molecules adsorbed on an aggregate of silver nanoparticles. Approximately 1000 R6G molecules were adsorbed on each nanoparticle and there were approximately 300 nanoparticles in the confocal laser spot (~3 x $10^5$ molecules probed). Because the absorption band of the analyte was in resonance with the excitation frequency, excited-state photodecomposition can occur.[31] The gradual progression from the narrow SERS peaks (<20 $cm^{-1}$ FWHM) of the intact R6G to the broad SERS peaks (>100 $cm^{-1}$ FWHM) of the photoproduct is observed. The final SERS spectrum (t = 30.00 s) is a sum of SERS spectra from intact R6G and R6G photoproduct(s). The photoproduct's two major SERS peaks at 1592 $cm^{-1}$ and 1340 $cm^{-1}$ are labeled in Figure 2.

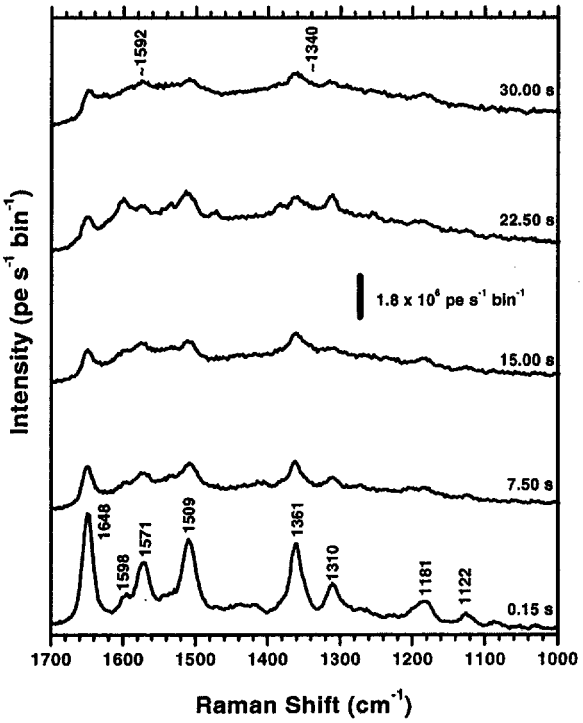


**Figure 2.** Bulk ensemble-averaged photodecomposition SERS spectra of R6G on silver nanoparticles. Five SERS spectra that highlight spectral changes are displayed with elapsed time noted. The scale bar represents 1.8 x $10^6$ pe/(s·bin). There are 2.3 $cm^{-1}$/bin. The R6G concentration was 20 x $10^{-8}$ M corresponding to ~1000 R6G molecules per nanoparticle and there were ~300 nanoparticles in the laser spot. $\lambda_{ex}$ = 514.5 nm; $t_{int}$ = 100 ms; $t_{readout}$ = 50 ms; M = 5 x $10^{24}$ photons/(s· $cm^2$). Spectra are offset for clarity.

To determine the rate of the photochemical reaction, the disappearance of the 1648 $cm^{-1}$ R6G SERS peak was monitored because it is virtually free of interference from SERS bands of the photoproduct(s). The area of this peak ($A_{1648}$), which is proportional to the concentration of intact R6G, was plotted as a function of time (t) as shown in Figure 3. The following exponential decay function was used to determine the photochemical rate constant ($k$) where t is time, B is the area of the 1648 $cm^{-1}$ peak at t = 0, and C is a constant used to correct for the background offset:

$$A_{1648} = Be^{-kt} + C \qquad (1)$$

The rate of photodecomposition of R6G ($k$) was determined under the set of experimental conditions described in Figure 2 to be 0.156 ± 0.007 $s^{-1}$. The photochemical rate constant was then determined in the same manner for a series of excitation powers. A log/log plot of the photochemical rate versus the excitation power yields a line with a slope of 0.9 ± 0.1 with a correlation coeffecient (R) of 0.98 (data not shown) demonstrating that the photodestruction is a first-order process.

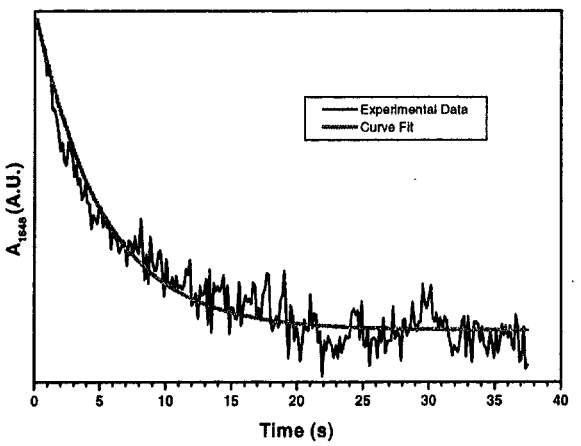


**Figure 3.** Bulk photodecomposition of R6G on silver nanoparticles. The area of the 1648 $cm^{-1}$ R6G peak ($A_{1648}$) is plotted vs. time. The R6G concentration is 20 x $10^{-8}$ M corresponding to ~ 1000 R6G molecules per nanoparticle. $\lambda_{ex}$ = 514.5 nm; $t_{int}$ = 100 ms; $t_{readout}$ = 50 ms; M = 5 x $10^{24}$ photons/(s· $cm^2$). The experimental data was fitted using Equation (1) with a reduced chi-squared value of 0.73. A photochemical rate constant ($k$) of 0.156 ± 0.007 $s^{-1}$ was determined from the fit.

A photodecomposition quantum yield ($\phi_d$) has been used to assess the photostability of fluorescent dyes.[32] This value is defined as the fraction of absorbed photons that cause a photodestruction event, and typically ranges from $10^{-5}$ to $10^{-7}$ for relatively photostable dye molecules in solution. A similar value can be calculated for the photostability of R6G on silver ($\phi_{dSERS}$) using the experimentally determined SERS photochemical rate constant ($k$) and the photon excitation rate ($k_{ex}$). $k_{ex}$ was calculated using Equation (2) where M is the irradiance of the laser spot in photons/(s·$cm^2$) and $\sigma_{SERS}$ is the surface-enhanced Raman scattering cross section. The

$\sigma_{SERS}$ replaces the absorption cross section that would be used to determine $k_{ex}$ for fluorescence. For R6G on silver, $\sigma_{SERS}$ has been estimated to be between $10^{-16}$ and $10^{-15}$ cm$^2$/molecule using 514.5-nm excitation.[2-5]

$$k_{ex} = M\sigma_{SERS} \quad (2)$$

With an M of 5 x $10^{24}$ photons/(s·cm$^2$), $k_{ex}$ ranges from 500 to 5000 MHz depending on the value of $\sigma_{SERS}$. $\phi_{dSERS}$ calculated from Equation (3) was in the range of $10^{-11}$ and $10^{-10}$ using $k$ obtained from the curve fit (Figure 3) and the calculated $k_{ex}$.

$$\phi_{dSERS} = k/k_{ex} \quad (3)$$

### 3.2 Single-Molecule SERS Spectra

In contrast to the ensemble-averaged SERS spectra described in Section 3.1, SERS spectra during the photodecomposition of a single R6G molecule are shown in Figure 4. At the single-molecule level, the transition from the intact R6G molecule to the R6G photoproduct can be seen to occur in discrete steps. In the beginning, fluctuations in the R6G spectral intensity were observed that have previously been reported (Figure 4a-e).[2,4,5] The intact R6G SERS spectra survived for approximately 12.90 s (Figure 4e) before it disappeared (Figure 4f). After a delay of approximately 3 seconds, a significantly altered SERS spectrum appeared (Figure 4g) and was followed by similar SERS spectra (Figure 4h-j). These spectra are believed to arise from the R6G photoproduct(s). The curiously long absence of SERS spectra (13.05 s to 15.90 s) before the observation of a photoproduct SERS spectrum was consistently observed with delays ranging from a few seconds to over ten seconds (50 total observations). The single-molecule SERS bands of the photoproduct were broader (~20 to 100 cm$^{-1}$ FWHM) than those observed for the intact R6G (<20 cm$^{-1}$ FWHM); however, the SERS spectra of single-molecule photoproducts were narrower than those found for the bulk ensemble-averaged spectra (>100 cm$^{-1}$ FWHM, Figure 2). The photoproduct SERS spectra also exhibited increased intensity fluctuations and a wide variability in the SERS peak frequencies.

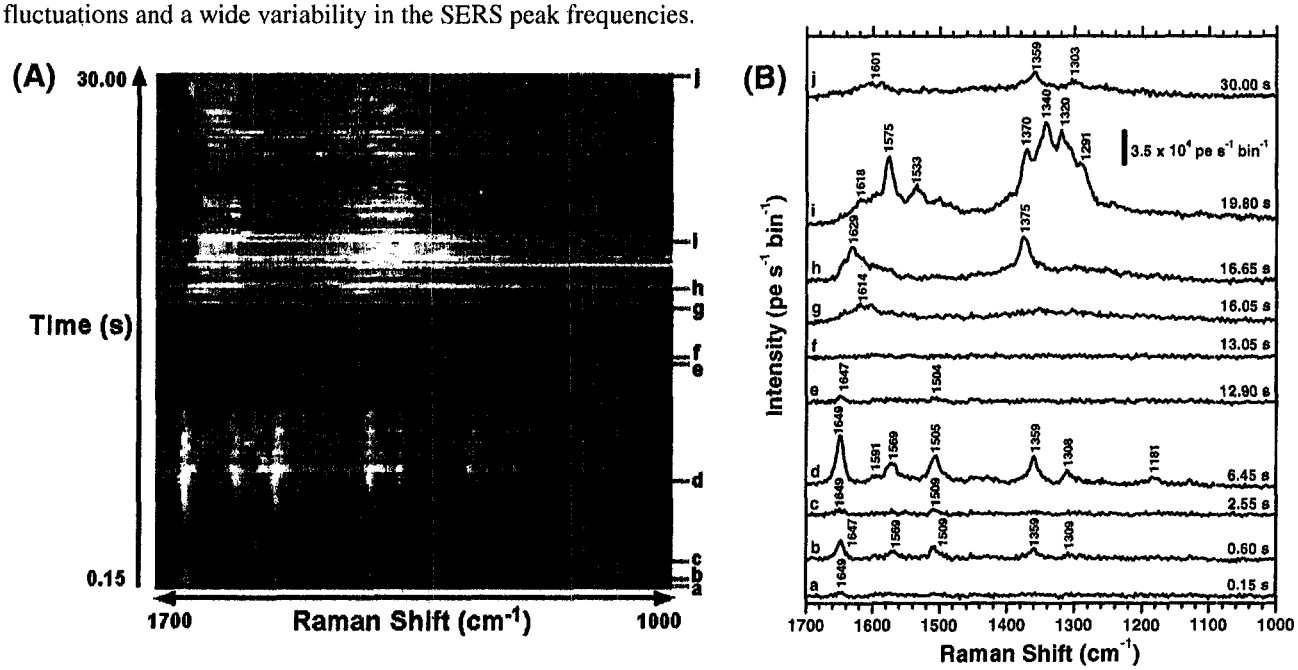


**Figure 4.** Photodecomposition of a single R6G molecule adsorbed on a silver nanoparticle. (**A**) Gray-scale intensity plot of 200 consecutive SERS spectra collected during the photodecomposition of a single R6G molecule. Intensity increases from black to white. Letters on the right side of the plot indicate the position of the corresponding SERS spectra shown in (B). Fluctuations in the SERS intensity can clearly be observed for both R6G and R6G photoproduct(s). The R6G SERS spectra (a to e) disappeared (f) and did not return after 13.05 s. After a delay of ~3 s it was followed by a photoproduct SERS spectrum (g) at 16.05 s. Significant changes in the SERS peak frequencies were observed in both R6G and photoproduct(s) SERS spectra. (**B**) Ten selected SERS spectra (from the 200 spectra in A) are displayed to highlight spectral changes. The letters correspond to the letters in (A) and the acquisition time of each spectrum is displayed on the right. The scale bar represents 3.5 x $10^4$ pe/(s·bin). There are 2.3 cm$^{-1}$/bin. Spectra are offset for clarity. Small changes in peak frequencies were observed in the R6G SERS spectra (a to e) and are attributed to changes in the orientation and local environment. Larger changes in the photoproduct SERS spectra (g to j) were observed and are attributed to changes in orientation, local environment, and the formation of additional photoproducts. Spectra were obtained under the following experimental conditions: R6G concentration was 20 x $10^{-12}$ M corresponding to ~ 0.1 R6G molecules per nanoparticle. $\lambda_{ex}$ = 514.5 nm; $t_{int}$ = 100 ms; $t_{readout}$ = 50 ms; M = 5 x $10^{24}$ photons/(s·cm$^2$).

The photochemical rate constant ($k$) was calculated using the survival times ($t_{survival}$) obtained for individual R6G molecules on silver. A similar method has been used to determine photobleaching rates for fluorescent molecules using LIF.[16b,17] The $t_{survival}$ of a single molecule was defined as the time when the R6G SERS spectrum dropped to the background level and was followed by a subsequent photoproduct SERS spectrum. Figure 5 shows a histogram of compiled survival times for fifty individual R6G molecules. The data were fitted to Equation (1), with C constrained to zero, and a rate constant of $0.13 \pm 0.02$ s$^{-1}$ was obtained from the fit. Because of the sparse nature of the data, $k$ was also calculated using a maximum likelihood estimator (MLE) method[33] to verify the results obtained from the least squares fit. Since all the observed R6G molecules photodecomposed during the observation time, $k$ was determined using Equation (4) where N is the number of observed events divided by the sum of $t_{survival}$.

$$k = N/\Sigma\, t_{survival} \qquad (4)$$

The MLE method yielded a $k = 0.16 \pm 0.02$ s$^{-1}$ that is in agreement with the value obtained from the least squares fit (Figure 5). $\phi_{dSERS}$ was then calculated with Equation (3) to be between $10^{-10}$ and $10^{-11}$ and is in good agreement with the values obtained from ensemble-averaged measurements (Section 3.1).

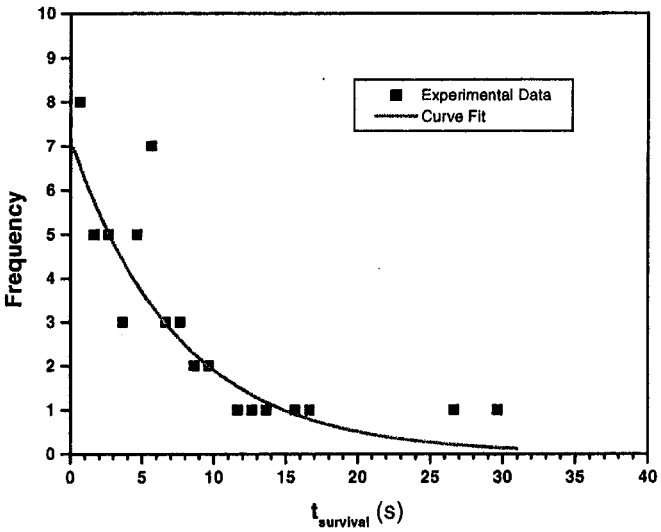


**Figure 5.** Histogram of individual survival times (squares). The data were binned using 1-s intervals and were fitted to Equation (1) with C constrained to zero (reduced chi-squared = 0.34). $k$ was determined to be $0.13 \pm 0.02$ s$^{-1}$ from the fit. The following experimental conditions were used for all 50 samples observed: R6G concentration was 20 x $10^{-12}$ M corresponding to ~ 0.1 R6G molecules per nanoparticle. $\lambda_{ex}$ = 514.5 nm; $t_{int}$ = 100 ms; $t_{readout}$ = 50 ms; M = 5 x $10^{24}$ photons/(s·cm$^2$).

## 4. DISCUSSION

### 4.1 Identification of R6G Photoproduct

The photoproduct SERS spectrum can be obtained either from an ensemble-averaged SERS spectrum that has the intact R6G spectrum subtracted out, or by adding a number of single-molecule R6G photoproduct SERS spectra (Figure 6). For simplicity, the identification of the R6G photoproduct was determined from these spectra that show broad peaks at 1592 cm$^{-1}$ and 1340 cm$^{-1}$ because of the complexity and variety of the single-molecule R6G photoproduct SERS spectra. However, the individual photoproducts could conceivably be identified using molecular models for SERS.[34] The SERS spectra shown in Figure 6 have been attributed to graphitic carbon.[35,36] Highly ordered macroscopic graphite crystals exhibit a narrow Raman band at 1575 cm$^{-1}$. This is attributed to in-plane atomic displacement and is of $E_{2g}$-symmetry. This band shifts slightly to higher frequencies (~1590 cm$^{-1}$) for very small graphite crystals. A Raman peak at approximately 1355 cm$^{-1}$ arises from the symmetry forbidden $A_{1g}$ mode of small crystallites or boundaries found in larger crystals. The ratio of the intensities of these two peaks can be used to estimate the size of the graphitic carbon photoproduct. Using the linear relationship developed by Tuinstra and Koenig,[35] we conservatively estimate the graphite

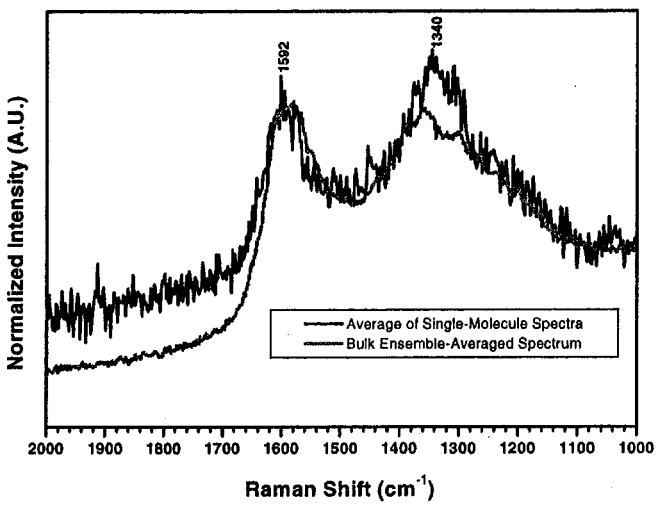


**Figure 6.** SERS spectra of R6G photoproduct(s). The solid line is a sum of 500 individual R6G photoproduct(s) SERS spectra. The gray line is from an ensemble-averaged measurement with the intact R6G SERS spectrum subtracted. For ease of comparison, both spectra are normalized to the 1592 cm$^{-1}$ peak.

fragments to be less than 5 nm in diameter. Our spectra with peaks at 1592 $cm^{-1}$ and 1340 $cm^{-1}$ are also consistent with the presence of extremely small graphite fragments. The individual R6G photoproduct(s) (Figure 4g-j) are believed to be various forms of graphitic carbon fragments that are the result of excited-state photochemical reaction(s) of R6G.

We were initially concerned that the observed graphitic carbon SERS spectrum could be the result of either carbon contamination[37] or possibly the citrate ions used to stabilize the colloidal nanoparticles.[38] However, blank samples under the same conditions yielded no detectable graphitic carbon SERS spectra. Additionally, the SERS spectrum of citrate ions consists of a weak peak at 1580 $cm^{-1}$ (carboxylate group asymmetric stretch) and a strong peak at 1415 $cm^{-1}$ (carboxylate symmetric stretch). Therefore, we have excluded carbon contamination and citrate ions as possible sources of the observed graphitic carbon SERS spectrum.

### 4.2 Photodecomposition Reaction Pathway

A striking difference between the ensemble-averaged and single-molecule data sets is the appearance of "off" times in the single-molecule SERS spectral traces (Figure 7A). This phenomenon has previously been reported for R6G on silver and has been only observed in single-molecule studies.[2,5] Brus and coworkers proposed that these "on" and "off" times are the result of a single R6G molecule adsorbing and desorbing from a SERS-active site repeatedly.[5] This

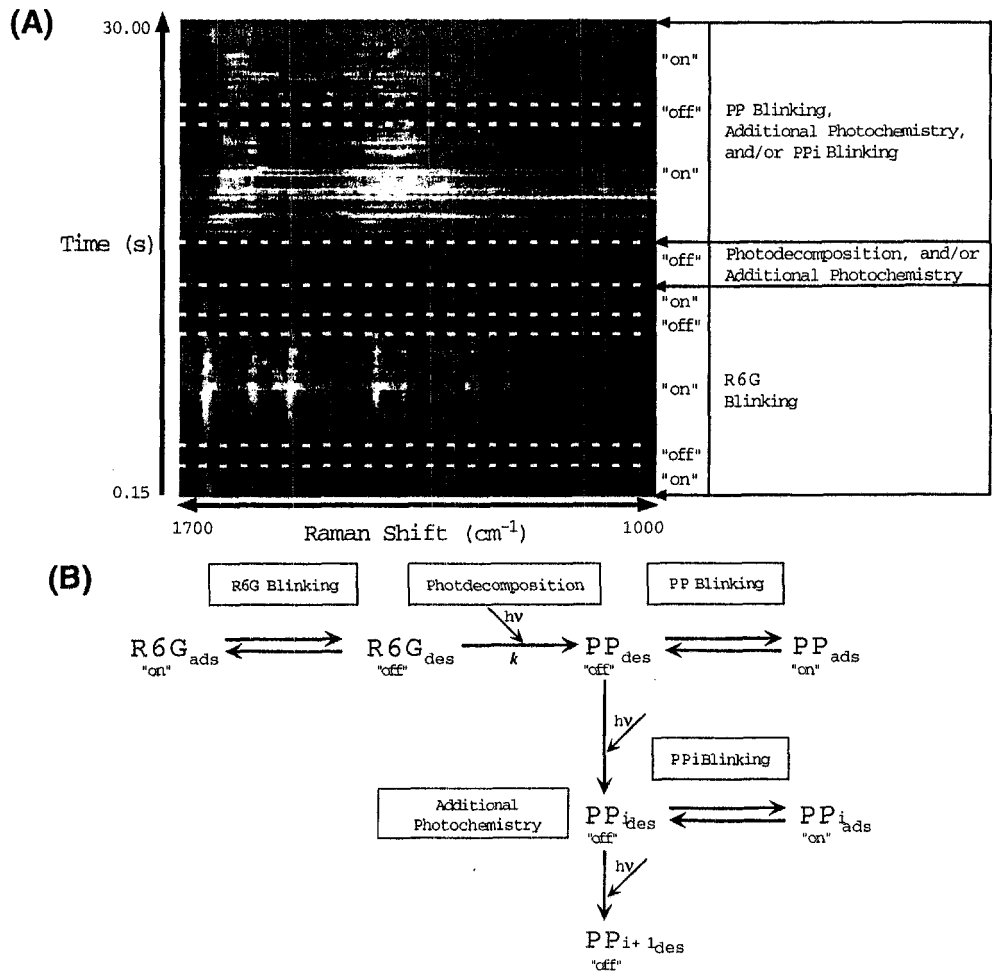


**Figure 7.** (**A**) The same gray-scale intensity plot in Figure 4 is shown with the reaction steps of the proposed photodecomposition pathway labeled on the right. Adsorption or "on" periods when SERS spectra were detected are labeled "on". Desorption or "off" periods when no SERS spectra were detected are labeled "off". Dashed lines indicate transitions between the "on" and "off" states. (**B**) A proposed pathway for the photodecomposition of R6G on silver. The blinking observed for the intact R6G SERS spectra is explained by reversible adsorption ($R6G_{ads}$) and desorption ($R6G_{des}$) of the R6G to and from a SERS-active site (R6G Blinking). Only when R6G is adsorbed to an active-site are R6G SERS spectra observed. During the desorption time, R6G may undergo irreversible excited-state photodecomposition (Photodecomposition). After photodecomposition, the photoproduct (PP) may readsorb to a SERS-active site (PP Blinking) or undergo additional photodecomposition (Additional Photochemistry) before readsorbing to a SERS-active (PP*i* Blinking). Upon adsorption, PP SERS spectra may be obtained.

behavior cannot be observed with ensemble-averaged measurements because the asynchronous adsorption and desorption of many molecules occurs simultaneously. When the R6G is slightly removed from the surface during these "off" or desorption times, it is more susceptible to excited-state photoreactions. This is because the local electromagnetic field is enhanced and the R6G molecular excited-states are not as efficiently quenched by the metal surface.[21-24] Based on the adsorption/desorption "blinking" theory and the model of surface-enhanced photochemistry, we propose a pathway by which the photodecomposition of R6G occurs during this desorption or "off" time and the graphitic carbon photoproduct (PP) SERS spectra are obtained when the PP adsorbs to a SERS-active site.

Figure 7B outlines the proposed photodecomposition pathway for R6G on silver and Figure 7A relates the proposed pathway to our single-molecule SERS data. The first step in the pathway involves the reversible adsorption and desorption of R6G to and from a SERS-active site (Figure 7B, R6G Blinking). When chemisorbed to an active-site ($R6G_{ads}$), a strong SERS spectrum is obtained because both chemical and electromagnetic enhancements are active.[2,5,6] Upon desorption ($R6G_{des}$), chemical enhancement ceases while electromagnetic enhancement is diminished. The molecule may move onto a layer of condensate or molecular ions such as citrate that act as a spacer layer. No SERS spectrum is detected because of the decrease in enhancement and the period is said to "off". It should be stated that although a diminished electromagnetic field enhancement may be sufficient to obtain a SERS spectrum from a large ensemble of desorbed species, the loss of chemical enhancement renders a single molecule undetectable with current instrument limitations. The $R6G_{des}$ is able to readsorb to the SERS-active site before photodecomposing and thus another R6G SERS spectrum can be obtained (Figure 7A, R6G Blinking). However, the $R6G_{des}$ can undergo irreversible excited-state photodecomposition in the desorbed state (Figure 7A, Photodecomposition). After photodecomposition, the PP can either adsorb to a SERS-active site to yield a PP SERS spectrum (Figure 7A, PP Blinking) or undergo further photodestruction (Figure 7A, Additional Photochemistry) before adsorbing and yielding a PP*i* SERS spectrum (Figure 7A, PP*i* Blinking). The presence of an "off" time prior to the appearance of the first PP SERS spectrum (Figure 4 and Figure 7B) is consistent with photodecomposition occurring in the desorbed state. However, the length of this "off" time (~seconds) is surprisingly long and warrants further study.

### 4.3 Inhomogeneous Broadening of Photoproduct SERS Spectra

Another difference between the ensemble-averaged and single-molecule spectra was in the SERS linewidths of the graphitic carbon photoproduct(s). Single-molecule photoproduct SERS spectra were narrower (~20 to 100 $cm^{-1}$ FWHM, Figure 4) than the bulk ensemble-averaged spectra (>100 $cm^{-1}$ FWHM, Figure 6). However, when single-molecule photoproduct spectra are added together, the result is an ensemble-like spectrum (Figure 6). This is consistent with an inhomogeneously broadened bulk ensemble-averaged photoproduct SERS spectrum due to a distribution of photoproducts in varying surface environments and orientations.[39]

An additional finding was that the photoproduct(s) exhibited greater temporal fluctuations in SERS intensity compared to R6G (data not shown); we attribute this to a difference in the strength of adsorption of R6G and graphitic carbon to silver. R6G adsorbs strongly to silver in the presence of chloride ions via a Ag-N bond ($|\Delta H_{ads}| = 65$ kJ/mol),[29] while graphitic carbon only weakly physisorbs to silver ($|\Delta H_{ads}| < 40$ kJ/mol). The difference in $\Delta H_{ads}$ means it is easier for graphitic carbon to desorb from the surface and, as a result, it blinks "on" and "off" faster than the chemisorbed R6G. This behavior inhomogeneously broadens the SERS spectra in two ways: (1) the photoproduct may undergo additional photodecomposition when it desorbs and thus its SERS spectrum will change; and (2) the photoproduct may rapidly change surface orientation resulting in an altered SERS spectrum.

### 4.4 Photostability of R6G on Silver Nanoparticles

It is important to note that the exceptional photostability of R6G on silver nanoparticles allows the photodecomposition reaction to occur on an observable time scale. The experimentally determined $\phi_{dSERS}$ is between $10^{-11}$ and $10^{-10}$ that is *3 to 4 orders* of magnitude more stable than the best fluorescent dye molecules in solution.[32] It should also be stated that there may be additional photodecomposition pathways that are too fast ($k > 1\ s^{-1}$) for our present system to monitor. However, the initial R6G ensemble-averaged SERS spectrum (Figure 2) did not display significant signs of photodecomposition that would be present if a faster reaction was occurring. Additionally, the fact that the ensemble-averaged ($k = 0.156 \pm 0.007\ s^{-1}$) and single-molecule ($k = 0.13 \pm 0.02\ s^{-1}$) photodecomposition rate constants are in agreement suggests that we are monitoring the dominant photodecomposition pathway.

## 5. CONCLUSIONS

This work demonstrates that single-molecule measurements can provide valuable new insights into chemical reactions by removing the mask of ensemble averaging. Based on the observed single-molecule SERS spectra, we postulate that the photodecomposition of R6G to graphitic carbon occurs when the R6G desorbs from the SERS-active site. The observation of long "off" times prior to the detection of photoproduct spectra is in accord with the hypothesis that the blinking behavior is caused by adsorption/desorption of R6G to and from SERS-active sites. This pathway is also consistent with theoretical predictions of photochemistry occurring slightly above the metal surface where a balance is struck between the enhanced electromagnetic field and the excited-state lifetime. These results further demonstrate how single-molecule SERS spectroscopy may be used to study chemical reactions at the single-molecule level. In the future, single-molecule SERS studies may be expanded to study biological or catalytic reactions to gain further insight into diverse reaction pathways.

## ACKNOWLEDGEMENTS

S.R.E. would like to acknowledge Los Alamos National Laboratory for a Director Funded Postdoctoral Fellowship. We would also like to thank John Fawcett for the loan of equipment.

## REFERENCES

1. For recent reviews: (a) Kneipp, K.; Kneipp, H.; Itzkan, I.; Dasari, R. R.; Feld, M. S. "Ultrasensitive Chemical Analysis by Raman Spectroscopy," *Chem. Rev.* **1999**, *99*, 2957. (b) Campion, A.; Kambhampati, P. "Surface-enhanced Raman scattering," *Chem. Soc. Rev.* **1998**, 27, 241.
2. (a) Nie, S.; Emory, S. R. "Probing single molecules and single nanoparticles by surface-enhanced Raman scattering," *Science* **1997**, 275, 1102. (b) Krug II, J. T.; Wang, J. D.; Emory, S. R.; Nie, S. "Efficient Raman enhancement and intermittent light emission observed in single gold nanocrystals," *J. Am. Chem. Soc.* **1999**, *121*, 9208.
3. (a) Kneipp, K.; Wang, Y.; Kneipp, H.; Perelman, L. T.; Itzkan, I.; Dasari, R. R.; Feld, M. S. "Single molecule detection using surface-enhanced Raman scattering (SERS)," *Phys. Rev. Lett.* **1997**, 78, 1667. (b) Kneipp, K.; Wang, Y.; Kneipp, H.; Itzkan, I.; Dasari, R. R.; Feld, M. S. "Population pumping of excited vibrational states by spontaneous surface-enhanced Raman scattering," *Phys. Rev. Lett.* **1996**, *76*, 2444. (c) Kneipp, K.; Kneipp, H.; Kartha, V. B.; Manoharan, R.; Deinum, G.; Itzkan, I.; Dasari, R. R.; Feld, M. S. "Detection and identification of a single DNA base molecule using surface-enhanced Raman scattering (SERS)," *Phys. Rev. E* **1998**, *57*, R6281.
4. Xu, H.; Bjerneld, E. J.; Kall, M.; Borjesson, L. "Spectroscopy of single hemoglobin molecules by surface enhanced Raman scattering," *Phys. Rev. Lett.* **1999**, *83*, 4357.
5. Michaels, A. M.; Nirmal, M.; Brus, L. E. "Surface enhanced Raman spectroscopy of individual Rhodamine 6G molecules on large Ag nanocrystals," *J. Am. Chem. Soc.* **1999**, *121*, 9932.
6. For general SERS reviews: (a) Moskovits, M. "Surface-enhanced spectroscopy," *Rev. Mod. Phys.* **1985**, *57*, 783. (b) Otto, A.; Mrozek, I.; Grahorn, B.; Akemann, W. "Surface-enhanced Raman scattering" *J. Phys. Condens. Matt.* **1992**, *4*, 1143. (c) Schatz, G. C. "Theoretical studies of surface-enhanced Raman scattering" *Acc. Chem. Res.***1984**, *17*, 370. (d) Vo-Dinh, T. "Surface-enhanced Raman spectroscopy using metallic nanostructures," *Trends Anal. Chem.* **1998**, *17*, 557.
7. (a) Emory, S. R.; Haskins, W. E.; Nie, S. "Direct observation of size-dependent optical enhancement in single metal nanoparticles," *J. Am. Chem. Soc.* **1998**, 120, 8009. (b) Emory, S. R.; Nie, S. "Screening and enrichment of metal nanoparticles with novel optical properties," *J. Phys. Chem. B* **1998**, 102, 493.
8. (a) Trautman, J. K.; Macklin, J. J.; Brus, L. E.; Betzig, E. "Near-field spectroscopy of single molecules at room temperature," *Nature* **1994**, *369*, 40. (b) Ambrose, W. P.; Goodwin, P. M.; Martin, J. C.; Keller, R. A. "Alterations of single-molecule fluorescence lifetimes in near-field optical microscopy," *Science* **1994**, *265*, 364. (c) Lu, H. P.; Xie, X. S. "Single-molecule spectral fluctuations at room temperature," *Nature (London)* **1997**, *385*, 143.
9. Dickson, R. M.; Cubitt, A. B.; Tsien, R. Y.; Moerner, W. E. "On/off blinking and switching behaviour of single molecules of green fluorescent protein," *Nature (London)* **1997**, *388*, 355.
10. (a) Vanden Bout, D. A.; Yip, W.-T.; Hu, D.; Fu, D.-K.; Swager, T. M.; Barbara, P. F. "Discrete intensity jumps and intramolecular electronic energy transfer in the spectroscopy of single conjugated polymer molecules," *Science* **1997**, *277*, 1074. (b) Yip, W.-T.; Hu, D.; Yu, J.; Vanden Bout, D. A.; Barbara, P. F. "Classifying the photophysical dynamics of single- and multiple-chromophoric molecules by single molecule spectroscopy," *J. Phys. Chem. A* **1998**, *102*, 7564.
11. Nirmal, M.; Dabbousi, B. O.; Bawendi, M. G.; Macklin, J. J.; Trautman, J. K.; Harris, T. D.; Brus, L. E. "Fluorescence intermittency in single cadmium selenide nanocrystals," *Nature* **1996**, *383*, 802.
12. S. A. Empedocles, S. A.; Bawendi, M. G. "Quantum-confined stark effect in single CdSe nanocrystallite quantum dots," *Science* **1997**, *278*, 2114.
13. Blanton, S. A.; Hines, M. A.; Guyot-Sionnest, P. "Photoluminescence wandering in single CdSe nanocrystals," *Appl. Phys. Lett.* **1996**, *69*, 3905.
14. Wazawa, T.; Ishii, Y.; Funatsu, T.; Yanagida, T. "Spectral fluctuation of a single fluorophore conjugated to a protein molecule," *Biophys. J.* **2000**, *78*, 1561.

15. Talaga, D. S.; Lau,W. L.; Roder, H.; Tang, J. Y.; Jia, Y. W.; DeGrado, W. F.; Hochstrasser, R. M. "Dynamics and folding of single two-stranded coiled-coil peptides studied by fluorescent energy transfer confocal microscopy," *Proc. Nat. Acad. Sci. (U.S.A.)* **2000**, *97*, 13021.
16. (a) Edman, L.; FoldesPapp, Z.; Wennmalm , S.; Rigler, R. "The fluctuating enzyme: a single molecule approach," *Chem. Phys.* **1999**, *247*, 11. (b) Wennmalm, S.; Rigler, R. "On death numbers and survival times of single dye molecules," *J. Phys. Chem. B* **1999**, *103*, 2516.
17. Wu, M.; Goodwin, P. M.; Ambrose, W. P.; Keller, R. A. "Photochemistry and fluorescence emission dynamics of single molecules in solution: B-phycoerythrin," *J. Phys. Chem.* **1996**, *100*, 17406.
18. Ambrose, W. P.; Goodwin, P. M.; Martin, J. C.; Keller, R. A. "Single molecule detection and photochemistry on a surface using near-field optical excitation," *Phys. Rev. Lett.* **1994**, *72*, 160.
19. Eggeling, C.; Wedengren, J.; Rigler, R., Seidel, C. A. M. "Photobleaching of fluorescent dyes under conditions used for single-molecule detection: evidence of two-step photolysis," *Anal. Chem.* **1998**, *70*, 2651.
20. Ying, L.; Xie, X. S. "Fluorescence spectroscopy, exciton dynamics, and photochemistry of single allophycocyanin trimers," *J. Phys. Chem. B* **1998**, *50*, 10399.
21. Nitzan, A.; Brus, L. E. "Theoretical model for enhanced photochemistry on rough surfaces," *J. Chem. Phys.* **1981**, *75*, 2205.
22. Das, P.; Metiu, H. "Enhancement of molecular fluorescence and photochemistry by small metal particles," *J. Phys. Chem.* **1985**, *89*, 4680.
23. Goncher, G. M.; Parsons, C. A.; Harris, C. B. "Photochemistry on rough metal surfaces," *J. Phys. Chem.* **1984**, *88*, 4200.
24. (a) Jeong, D. H.; Suh, J. S.; Moskovits, M. "Photochemical reactions of phenazine and acridine adsorbed on silver colloid surfaces," *J. Phys. Chem. B.* **2000**, *104*, 7462. (b) Jeong, D. H.; Jang, N. H.; Suh, J. S.; Moskovits, M. "Photodecomposition of diazanaphthalenes adsorbed on silver colloid surfaces," *J. Phys. Chem. B.* **2000**, *104*, 3594. (c) Jang, N. H.; Suh, J. S.; Moskovits, M. "Effect of surface geometry on the photochemical reaction of 1,10-phenanthroline adsorbed on silver colloid surfaces," *J. Phys. Chem. B.* **1997**, *101*, 8279. (d) Suh, J. S.; Jang, N. H.; Jeong, D. H.; Moskovits, M. "Adsorbate photochemistry on a colloid surface: phthalazine on silver," *J. Phys. Chem.* **1996**, *100*, 805. (e) Suh, J. S.; Moskovits, M.; Shakhesemampour, J. "Photochemical decomposition at colloid surfaces," *J. Phys. Chem.* **1993**, *97*, 1678. (f) Wolkow, R. A.; Moskovits, M. "Enhanced photochemistry on silver surfaces," *J. Phys. Chem.* **1987**, *87*, 5858.
25. Jang, N. H.; Suh, J. S.; Moskovits, M. "Photochemical desorption of 4-vinylbenzoic acid adsorbed on silver colloid surfaces," *J. Phys. Chem. B.* **1997**, *101*, 1649.
26. (a) Suh, J. S.; Jeong, D. H.; Lee, M. S. "Effect of inhomogeneous broadening on the surface photochemistry of pthalazine," *J. Raman Spec.* **1999**, *30*, 595. (b) McMahon, J. J.; Gergel, T. J.; Otterson, D. M.; McMahon, C. R.; Kabbani, R. M. "Photochemical charge transfer excitation of trans-4-stilbazole at a silver electrode," *Surf. Sci.* **1999**, *440*, 357. (c) Kidd, R. T.; Meech, S. R.; Lennon, D. "Enhanced photodesorption of NO on roughened silver surfaces," *Chem. Phys. Lett.* **1996**, *262*, 142. (d)Azim, S. A.; El-Daly, H. A.; El-Daly, S. A.; Abou-Zeid, Kh. A.; Ebeid, E. M.; Heldt, J. R. "Energy transfer and photodecomposition of anthracene laser dyes," *J. Chem. Soc. Faraday Trans.* **1996**, *92*, 2685.
27. (a) Garoff, S.: Weitz, D. A.; Alverez, M. S. "Photochemistry of molecules adsorbed on silver-island films: effects of the spatially inhomogeneous environment," *Chem. Phys. Lett.* **1982**, *93*, 283. (b) Waldeck, D. H.; Alivisatos, A. P.; Harris, C. B. "Nonradiative damping of molecular electronic excited states by metal surfaces," *Surf. Sci.* **1985**, *158*, 103.
28. Lee, P. C.; Meisel, D. "Adsorption and surface-enhanced Raman of dyes on silver and gold sols" *J. Phys. Chem.* **1982**, *86*, 3391.
29. Hildebrandt, P.; Stockburger, M. "Surface-enhanced resonance Raman spectroscopy of Rhodamine 6G adsorbed on colloidal silver," *J. Phys. Chem.* **1984**, *88*, 5935.
30. Keller, H. E. "Objective lenses for confocal microscopy," In *Handbook of Confocal Microscopy*, Pawley, J. B., Ed.; Plenum Press: New York, **1995**, 111.
31. (a) George, N. A.; Aneeshkumar, B.; Radhakrishnan, P.; Vallabhan, C. P. G. "Photoacoustic study on photobleaching of Rhodamine 6G doped in poly(methyl methacrylate)," *J. Phys. D: Appl. Phys.* **1999**, *32*, 1745. (b) Mialocq, J. C.; Hebert, Ph.; Armand, X.; Bonneau, R.; Morand, J. P. "Photophysical and photochemical properties of Rhodamine 6G in alcoholic and aqueous sodium dodecylsuphate micellar solutions," *J. Photochem. Photobiol. A: Chem.* **1991**, *56*, 323.
32. Soper, S. A.; Nutter, H. L.; Keller, R. A.; Davis, L. M.; Shera, E. B. "The photophysical constants of several fluorescent dyes pertaining to ultrasensitive fluorescence spectrscopy," *Photochem. Photobiol.* **1993**, *57*, 972.
33. Tellinghuisen, J.; Wilkerson, C. W., Jr. "Bias and precision in the estimation of exponential decay parameters from sparse data," *Anal. Chem.* **1993**, *65*, 1240.
34. Sagmuller, B.; Freunscht, P.; Schneider, S. "The assignment of the vibrations of substituted mercaptotetrazoles based on quantum chemical calculations," *J. Mol. Struct.* **1999**, *483*, 231.
35. Tuinstra, F.; Koenig, J. L. "Raman spectrum of graphite," *J. Chem. Phys.* **1970**, *53*, 1126.
36. (a) Moyer, P. J.; Schmidt, J.; Eng, L. M.; Meixner, A. J. "Surface-enhanced Raman scattering spectroscopy of single carbon domains on individual Ag nanoparticles on a 25 ms time scale," *J. Am. Chem. Soc.* **2000**, *122*, 5409. (b) Kudelski, A.; Pettinger, B. "SERS on carbon chain segments: monitoring locally surface chemistry," *Chem. Phys. Lett.* **2000**, *321*, 356.
37. (a) Taylor, C. E.; Garvey, S. D.; Pemberton, J. E. "Carbon contamination at silver surfaces: surface preparation procedures evaluated by Raman spectrscopy and x-ray photoelectron spectroscopy," *Anal. Chem.* **1996**, *68*, 2401. (b) Norrod, K. L.; Rowlen, K. L. "Removal of carbonaceous contamination from SERS-active silver by self-assembly of decanethiol," *Anal. Chem.* **1998**, *70*, 4218.
38. (a) Kerker, M.; Siiman, O.; Bumm, L. A.; Wang, D.-S. "Surface enhanced Raman scattering (SERS) of citrate ion adsorbed on colloidal silver," *Appl. Opt.* **1980**, *19*, 3253. (b) Siiman, O.; Bumm, L. A.; Callaghan, R., Blatchford, C. G.; Kerker, M. "Surface-enhanced Raman scattering by citrate on colloidal silver," *J. Phys. Chem.* **1983**, *87*, 1014.
39. Kudelski, A.; Pettinger, B. "SERS on carbon chain segments: monitoring locally surface chemistry," *Chem. Phys. Lett.* **2000**, *321*, 356.